# Comparative study of three-nucleon force models in $A = 3, 4$ systems

A. Kievsky,[1,*] M. Viviani,[1] L. Girlanda,[2] and L. E. Marcucci[2]
[1]*Istituto Nazionale di Fisica Nucleare, Largo Pontecorvo 3, I-56127 Pisa, Italy*
[2]*Dipartimento di Fisica, Università di Pisa, Largo Pontecorvo 3, I-56127 Pisa, Italy*
(Received 5 February 2010; published 28 April 2010)

Using modern nucleon-nucleon interactions in the description of $A = 3, 4$ nuclei, it is not possible to reproduce both the three- and the four-nucleon binding energies simultaneously. This is one manifestation of the necessity of including a three-nucleon force in the nuclear Hamiltonian. In this paper we perform a comparative study of some widely used three-nucleon force models. We analyze their capability to describe the aforementioned binding energies as well as the $n$-$d$ doublet scattering length. The correct description of these quantities can be considered a stringent requirement for a nuclear Hamiltonian containing two- and three-nucleon interaction terms. As we show, this requirement is not fulfilled by several of the models available in the literature. To satisfy it, we propose modifications in the parametrization of the three-nucleon forces and we study their effects on a few selected $N$-$d$ low-energy scattering observables.

DOI: 10.1103/PhysRevC.81.044003 PACS number(s): 21.30.−x, 21.45.Ff, 27.10.+h

## I. INTRODUCTION

Realistic nucleon-nucleon ($NN$) potentials reproduce the experimental $NN$ scattering data up to energies of 350 MeV with a $\chi^2$ per datum close to 1. However, the use of these potentials in the description of three- and four-nucleon bound and scattering states gives a $\chi^2$ per datum much larger than 1 (see, e.g., Ref. [1]). To improve that situation, different three-nucleon force (TNF) models have been introduced so far. Widely used in the literature are the Tucson-Melbourne (TM) and the Urbana IX (URIX) models [2,3]. These models are based on the exchange mechanism of two pions between three nucleons. The TM model has been revisited within a chiral symmetry approach [4], and it has been demonstrated that the contact term present in it should be dropped. This new TM potential, known as TM′, has been subsequently readjusted [5]. The final operatorial structure coincides with the one given in the TNF of Brazil derived many years ago [6]. TNF models based on $\pi\rho$ and $\rho\rho$ meson exchange mechanisms have also been derived [7] and their effects have been studied in the triton binding energy [8]. More recently, TNFs have been derived [9] using a chiral effective field theory at next-to-next-to-leading order. A local version of these interactions (hereafter referred as N2LOL) is given in Ref. [10]. At this particular order, the TNF has two unknown constants that have to be determined. More in general, all the models contain a certain number of parameters that fix the strength of the different terms that compose the interaction. It is a common practice to determine these parameters from the three- and four-nucleon binding energies. In the chiral effective field theory there is a consistent derivation of two- and three-nucleon interactions and some of the low-energy constants entering in the TNF are fixed already from the $NN$ data. On the contrary, the parametrization of the TM′ and URIX interactions have been determined in association with specific $NN$ potentials. Therefore, their parametrizations could change when used with different $NN$ potentials because different $NN$ potentials predict different $A = 3, 4$ binding energies.

The $n$-$d$ doublet scattering length ${}^2a_{nd}$ can give valuable information. In principle, this quantity is correlated, to some extent, with the $A = 3$ binding energy through the so-called Phillips line [11,12]. However the presence of TNFs of the type studied here breaks this correlation. Therefore ${}^2a_{nd}$ emerges as an independent observable that can be used to evaluate the capability of the interaction models to describe the low-energy region. Owing to the lack of excited states in the $A = 3$ system, the zero-energy state is the first one above the ground state. In the case of $n$-$d$ scattering at zero energy, the $J = \frac{1}{2}^+$ state is orthogonal to the triton ground state, and for this reason, the wave function presents a node in the relative distance between the incident nucleon and the deuteron. The position of the node is related to the scattering length and it is also sensitive to the relation between the overall attraction and repulsion of the interaction. Several of the realistic $NN$ potentials underestimate the triton binding energy. Adding a TNF, which in general can include an attractive as well as a repulsive component, with a strength fixed, for example, to reproduce the triton binding energy, the balance between the overall attraction and repulsion of the interaction changes with respect to that produced by the $NN$ potential alone. And, as we show, this leads to different predictions of ${}^2a_{nd}$ and the $\alpha$-particle binding energy $B({}^4\mathrm{He})$. An analysis of the parametrization of a chiral TNF, to describe the triton binding energy $B({}^3\mathrm{H})$, $B({}^4\mathrm{He})$, and ${}^2a_{nd}$, has been performed in Ref. [9]. A similar analysis has not been done for the local models URIX, TM′, and N2LOL, as only the three- or four-body binding energy has been considered in the determination of their parametrization, and not ${}^2a_{nd}$.

In Ref. [13] results for different combinations of $NN$ interactions plus TNF models are given. We report the results for the quantities of interest in Table I. From the table, we can see that the models are not able to describe simultaneously the $A = 3, 4$ binding energies and ${}^2a_{nd}$. Triggered by this fact, in this paper we make a comparative study of the aforementioned TNF models. To this end we use the AV18 [14] as the reference $NN$ interaction and the three-nucleon interaction

*kievsky@pi.infn.it

 

TABLE I. Triton and $^4$He binding energies $B$ (MeV) and doublet scattering length $^2a_{nd}$ (fm) calculated using the AV18 and the N3LO-Idaho two-nucleon potentials and the AV18 + URIX, AV18 + TM′, and N3LO-Idaho + N2LOL two- and three-nucleon interactions. Experimental values are given in the last row.

| Potential | $B(^3\mathrm{H})$ | $B(^4\mathrm{He})$ | $^2a_{nd}$ |
|---|---|---|---|
| AV18 | 7.624 | 24.22 | 1.258 |
| N3LO-Idaho | 7.854 | 25.38 | 1.100 |
| AV18 + TM′ | 8.440 | 28.31 | 0.623 |
| AV18 + URIX | 8.479 | 28.48 | 0.578 |
| N3LO-Idaho + N2LOL | 8.474 | 28.37 | 0.675 |
| Exp. | 8.482 | 28.30 | $0.645 \pm 0.003 \pm 0.007$ |

models are added to it. Parametrizations of the URIX and TM′ models already exist in conjunction with the AV18 potential. Conversely the N2LOL TNF has been constructed using the N3LO-Idaho potential from Ref. [15]. So, in the first step, we have adapted its parametrization to reproduce, in conjunction with the AV18 interaction, $B(^3\mathrm{H})$. Successively, we study the sensitivity of different parametrizations in the description of $B(^4\mathrm{He})$ and $^2a_{nd}$. Selecting those parametrizations that predict these three quantities close to their experimental values, we study some polarization observables in $p$-$d$ scattering at $E_{\mathrm{lab}} = 3$ MeV. As an interesting result, we have observed that the predictions of the different parametrizations fall in a narrow band that, in the case of the vector analyzing powers, has a different position for each model, indicating a sensitivity to the short-range structure of the TNF.

All calculations have been done using the hyperspherical harmonics method as developed by some of the authors to describe bound and scattering states in $A = 3, 4$ systems [16–19] in configuration space or in momentum space [20,21] (for a recent review see Ref. [13]). The paper is organized as follows. In the next section we introduce the TNF models in configuration space defining their parametrizations. In Sec. III we make a sensitivity study of the parametrization for each model looking at $B(^3\mathrm{H})$, $B(^4\mathrm{He})$, and $^2a_{nd}$. In Sec. IV we study $p$-$d$ polarization observables at $E_{\mathrm{lab}} = 3$ MeV for specific values of the parameters. The conclusions are given in Sec. V.

## II. THREE-NUCLEON FORCE MODELS

In Ref. [13] the description of bound states and zero-energy states for $A = 3, 4$ was reviewed in the context of the hyperspherical harmonics method. In Table I we report results for the triton and $^4$He binding energies as well as for the doublet $n$-$d$ scattering length $^2a_{nd}$ using the AV18 and the N3LO-Idaho NN potentials and using the following combinations of two- and three-nucleon interactions: AV18 + URIX, AV18 + TM′, and N3LO-Idaho + N2LOL. The results are compared to the experimental values also reported in Table I. Worthy of notice is the recent very accurate datum for $^2a_{nd}$ [22].

From Table I we may observe that only the results obtained using an interaction model that includes a TNF are close to the corresponding experimental values. In the case of the AV18 + TM′, the strength of the TM′ potential has been fixed to reproduce the $^4$He binding energy, and as can be seen from the table, the triton binding energy is underpredicted. Conversely, the strength of the URIX potential has been fixed to reproduce the triton binding energy, giving too much binding for $^4$He. The strength of the N2LOL potential has been fixed to reproduce simultaneously the triton and the $^4$He binding energies. In the three cases the predictions for the doublet scattering length are not in agreement with the experimental value, in particular, for the AV18 + URIX model.

Our intention is to study different parametrizations of the TNFs, to obtain, as closely as possible, a simultaneous description of the three quantities under observation. To this aim we give a brief description of the TM′ (or Brazil), URIX, and N2LOL models. Starting from the general TNF

$$W = \sum_{cyc} W(i, j, k), \tag{1}$$

a generic term can be put in the following form:

$$\begin{aligned} W(1,2,3) = {} & a W_a(1,2,3) + b W_b(1,2,3) + d W_d(1,2,3) \\ & + c_D W_D(1,2,3) + c_E W_E(1,2,3). \end{aligned} \tag{2}$$

Each term corresponds to a different mechanism and has a different operatorial structure. The first three terms arise from the exchange of two pions between three nucleons. The $a$ term comes from $\pi N$ $S$-wave scattering, whereas the $b$ term and $d$ term, which are the most important, come from $\pi N$ $P$-wave scattering. The specific form of these three terms in configuration space is the following:

$$\begin{aligned} W_a(1,2,3) = {} & -W_0(\boldsymbol{\tau}_1 \cdot \boldsymbol{\tau}_2)(\boldsymbol{\sigma}_1 \cdot \boldsymbol{r}_{31})(\boldsymbol{\sigma}_2 \cdot \boldsymbol{r}_{23}) y(r_{31}) y(r_{23}), \\ W_b(1,2,3) = {} & W_0(\boldsymbol{\tau}_1 \cdot \boldsymbol{\tau}_2)[(\boldsymbol{\sigma}_1 \cdot \boldsymbol{\sigma}_2) y(r_{31}) y(r_{23}) \\ & + (\boldsymbol{\sigma}_1 \cdot \boldsymbol{r}_{31})(\boldsymbol{\sigma}_2 \cdot \boldsymbol{r}_{23})(\boldsymbol{r}_{31} \cdot \boldsymbol{r}_{23}) t(r_{31}) t(r_{23}) \\ & + (\boldsymbol{\sigma}_1 \cdot \boldsymbol{r}_{31})(\boldsymbol{\sigma}_2 \cdot \boldsymbol{r}_{31}) t(r_{31}) y(r_{23}) \\ & + (\boldsymbol{\sigma}_1 \cdot \boldsymbol{r}_{23})(\boldsymbol{\sigma}_2 \cdot \boldsymbol{r}_{23}) y(r_{31}) t(r_{23})], \\ W_d(1,2,3) = {} & W_0(\boldsymbol{\tau}_3 \cdot \boldsymbol{\tau}_1 \times \boldsymbol{\tau}_2)[(\boldsymbol{\sigma}_3 \cdot \boldsymbol{\sigma}_2 \times \boldsymbol{\sigma}_1) y(r_{31}) y(r_{23}) \\ & + (\boldsymbol{\sigma}_1 \cdot \boldsymbol{r}_{31})(\boldsymbol{\sigma}_2 \cdot \boldsymbol{r}_{23})(\boldsymbol{\sigma}_3 \cdot \boldsymbol{r}_{23} \times \boldsymbol{r}_{31}) t(r_{31}) t(r_{23}) \\ & + (\boldsymbol{\sigma}_1 \cdot \boldsymbol{r}_{31})(\boldsymbol{\sigma}_2 \cdot \boldsymbol{r}_{31} \times \boldsymbol{\sigma}_3) t(r_{31}) y(r_{23}) \\ & + (\boldsymbol{\sigma}_2 \cdot \boldsymbol{r}_{23})(\boldsymbol{\sigma}_3 \cdot \boldsymbol{r}_{23} \times \boldsymbol{\sigma}_1) y(r_{31}) t(r_{23})], \end{aligned} \tag{3}$$

with $W_0$ an overall strength. The $b$ and $d$ terms are present in the three models, whereas the $a$ term is present in the TM′ and N2LOL but not in URIX. In the first two models, the radial functions $y(r)$ and $t(r)$ are obtained from the following function:

$$f_0(r) = \frac{12\pi}{m_\pi^3} \frac{1}{2\pi^2} \int_0^\infty dq q^2 \frac{j_0(qr)}{q^2 + m_\pi^2} F_\Lambda(q), \tag{4}$$

where $m_\pi$ is the pion mass and

$$\begin{aligned} y(r) &= \frac{1}{r} f_0'(r), \\ t(r) &= \frac{1}{r} y'(r). \end{aligned} \tag{5}$$

The cutoff function $F_\Lambda$ in the TM′ or Brazil models is taken as $F_\Lambda = [(\Lambda^2 - m_\pi^2)/(\Lambda^2 + q^2)]^2$. In the N2LOL model it is taken as $F_\Lambda = \exp(-q^4/\Lambda^4)$. The momentum cutoff $\Lambda$ is a parameter of the model fixing the scale of the problem in

momentum space. In the N2LOL, it has been fixed to $\Lambda = 500$ MeV, whereas in the TM′ model the ratio $\Lambda/m_\pi$ has been varied to describe the triton or $^4$He binding energy at fixed values of the constants $a$, $b$, and $d$. In the literature the TM′ potential has been used many times, with typical values around $\Lambda = 5m_\pi$.

In the URIX model the radial dependence of the $b$ and $d$ terms is given in terms of the functions

$$\begin{aligned} Y(r) &= (e^{-x}/x)\,\xi_Y, \\ T(r) &= [1 + (3/x) + (3/x^2)]Y(r)\xi_T, \end{aligned} \tag{6}$$

where $x = m_\pi r$ and the cutoff functions are defined as $\xi_Y = \xi_T = (1 - e^{-cr^2})$, with $c = 2.1$ fm$^{-2}$. This regularization has been used in the AV18 potential as well. Because the URIX model has been constructed in conjunction with the AV18 potential, the use of the same regularization was a choice of consistency. The relation between the functions $Y(r)$, $T(r)$ and those of the previous models is

$$\begin{aligned} Y(r) &= y(r) + T(r), \\ T(r) &= \frac{r^2}{3} t(r). \end{aligned} \tag{7}$$

With the definition given in Eq. (4), the asymptotic behavior of the functions $f_0(r)$, $y(r)$, and $t(r)$ is

$$\begin{aligned} f_0(r \to \infty) &\to \frac{3}{m_\pi^2}\frac{e^{-x}}{x}, \\ y(r \to \infty) &\to -\frac{3e^{-x}}{x^2}\left(1 + \frac{1}{x}\right), \\ t(r \to \infty) &\to \frac{3}{r^2}\frac{e^{-x}}{x}\left(1 + \frac{3}{x} + \frac{3}{x^2}\right). \end{aligned} \tag{8}$$

Note that with the normalization chosen for $f_0$, the functions $Y$ and $T$ defined from $y$ and $t$ and those defined in the URIX model coincide at large separation distances. Conversely, they have a different short-range behavior. Using the URIX $Y(r)$, $T(r)$ functions, the $a$ term has been included in the construction of the Illinois TNF model [23].

The last two terms in Eq. (2) correspond to a two-nucleon ($2N$) contact term with a pion emitted or absorbed ($D$ term) and to a three-nucleon ($3N$) contact interaction ($E$ term). Their local form, in configuration space, derived in Ref. [10], is

$$\begin{aligned} W_D(1,2,3) = W_0^D(\boldsymbol{\tau}_1 \cdot \boldsymbol{\tau}_2)\{&(\boldsymbol{\sigma}_1 \cdot \boldsymbol{\sigma}_2) \\ &\times [y(r_{31})Z_0(r_{23}) + Z_0(r_{31})y(r_{23})] \\ &+ (\boldsymbol{\sigma}_1 \cdot \boldsymbol{r}_{31})(\boldsymbol{\sigma}_2 \cdot \boldsymbol{r}_{31})t(r_{31})Z_0(r_{23}) \\ &+ (\boldsymbol{\sigma}_1 \cdot \boldsymbol{r}_{23})(\boldsymbol{\sigma}_2 \cdot \boldsymbol{r}_{23})Z_0(r_{31})t(r_{23})\}, \\ W_E(1,2,3) = W_0^E(\boldsymbol{\tau}_1 \cdot \boldsymbol{\tau}_2)&Z_0(r_{31})Z_0(r_{23}). \end{aligned} \tag{9}$$

The constants $W_0^D$ and $W_0^E$ fix the strength of these terms. In the case of the URIX model the $D$ term is absent, whereas the $E$ term is present without the isospin operatorial structure, and it has been included as purely phenomenological, without justifying its form from a particular exchange mechanism. Its radial dependence has been taken as $Z_0(r) = T^2(r)$. In the N2LOL model, the function $Z_0(r)$ is defined as

$$Z_0(r) = \frac{12\pi}{m_\pi^3}\frac{1}{2\pi^2}\int_0^\infty dq q^2 j_0(qr) F_\Lambda(q), \tag{10}$$

with the same cutoff function used before, $F_\Lambda(q) = \exp(-q^4/\Lambda^4)$. In the TM′ model the $D$ and $E$ terms are absent.

Each model is now identified from the values assigned to the different constants. Following Refs. [5] and [24], in the case of the TM′ model, the values of the constants are $a = -0.87\ m_\pi^{-1}$, $b = -2.58\ m_\pi^{-3}$, and $d = -0.753\ m_\pi^{-3}$; the strength $W_0 = (g m_\pi/8\pi m_N)^2\ m_\pi^4$ and the cutoff has been fixed to $\Lambda = 4.756\ m_\pi$, to describe correctly, associated with AV18, $B(^4\text{He})$. In Table I the calculations have been done using these values with $g^2 = 197.7$, $m_\pi = 139.6$ MeV, and $m_N/m_\pi = 6.726$ ($m_N$ is the nucleon mass) as given in the original derivation of the TM potential.

In the URIX model the $b$ and $d$ terms are present, however, at a fixed ratio based on the Fujita-Miyazawa diagram. The strength of these terms are $bW_0 = 4\ A_{2\pi}^{\text{PW}}$ and $d = b/4$, with $A_{2\pi}^{\text{PW}} = -0.0293$ MeV. The model includes a purely central repulsive term introduced to compensate the attraction of the previous term, which by itself would produce a large overbinding in infinite nuclear matter. It is defined as

$$W_E^{\text{URIX}}(1,2,3) = A_R T^2(r_{31})T^2(r_{23}), \tag{11}$$

with $A_R = 0.0048$ MeV.

In the N2LOL potential the constants of the $a$, $b$, $d$, $D$, and $E$ terms are defined as follows:

$$\begin{aligned} W_0 &= \frac{1}{12\pi^2}\left(\frac{m_\pi}{F_\pi}\right)^4 g_A^2 m_\pi^2, \\ W_0^D &= \frac{1}{12\pi^2}\left(\frac{m_\pi}{F_\pi}\right)^4 \left(\frac{m_\pi}{\Lambda_x}\right)\frac{g_A m_\pi}{8}, \\ W_0^E &= \frac{1}{12\pi^2}\left(\frac{m_\pi}{F_\pi}\right)^4 \left(\frac{m_\pi}{\Lambda_x}\right) m_\pi, \end{aligned} \tag{12}$$

with $a = c_1 m_\pi^2$, $b = c_3/2$, $d = c_4/4$, and $c_1 = -0.00081\ \text{MeV}^{-1}$, $c_3 = -0.0032\ \text{MeV}^{-1}$, and $c_4 = -0.0054\ \text{MeV}^{-1}$ taken from Ref. [15] (to be noted the minus sign in $c_4$ adopted here). The other two constants, $c_D = 1.0$ and $c_E = -0.029$, were determined in Ref. [10] from a fit to $B(^3\text{H})$ and $B(^4\text{He})$ using the N3LO-Idaho + N2LOL potential model. The numerical values of the constant entering in $W_0$, $W_0^D$, and $W_0^E$ are $m_\pi = 138$ MeV, $F_\pi = 92.4$ MeV, and $g_A = 1.29$, and the chiral symmetry breaking scale $\Lambda_x = 700$ MeV.

To analyze the different short-range structures of the TNF models, in Fig. 1 we compare the dimensionless functions $Z_0(r)$, $y(r)$, and $T(r)$ for the three models under consideration. In the TM′ model using the definition in Eq. (10) and using the corresponding cutoff function, we can define

$$\begin{aligned} Z_0^{\text{TM}}(r) &= \frac{12\pi}{m_\pi^3}\frac{1}{2\pi^2}\int_0^\infty dq q^2 j_0(qr)\left(\frac{\Lambda^2 - m_\pi^2}{\Lambda^2 + q^2}\right)^2 \\ &= \frac{3}{2}\left(\frac{m_\pi}{\Lambda}\right)\left(\frac{\Lambda^2}{m_\pi^2} - 1\right)^2 e^{-\Lambda r}. \end{aligned} \tag{13}$$

This function is shown as a dashed line in the first panel in Fig. 1. From the figure we can see that, in the case of the URIX

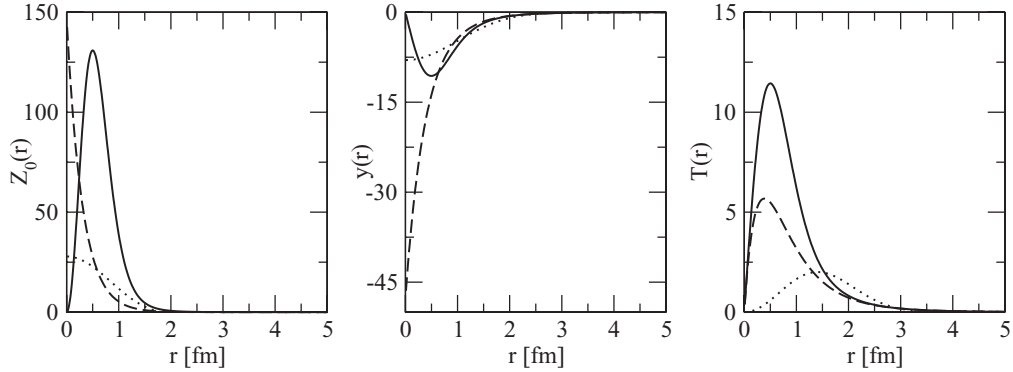


FIG. 1. $Z_0(r)$, $y(r)$, and $T(r)$ functions as functions of the interparticle distance $r$ for the URIX (solid line), TM′ (dashed line), and N2LOL (dotted line) models.

model, the functions $Z_0(r)$ and $y(r)$ go to zero as $r \to 0$. This is not the case for the other two models and is a consequence of the regularization choice of the $Y$ and $T$ functions adopted in the URIX.

## III. PARAMETRIZATION STUDY OF THE THREE-NUCLEON FORCES

In this section we study possible variations to the parametrization of the TNF models, to describe the $A = 3, 4$ binding energies and ${}^2a_{nd}$.

### A. Tucson-Melbourne force

We first study the TM′ potential and we would like to see whether, using the AV18 + TM′ interaction, it is possible to reproduce simultaneously the triton binding energy and the doublet $n$-$d$ scattering length for some values of the parameters. The $a$ term gives a very small contribution to these quantities, therefore, in the following analysis we maintain it fixed at the value $a = -0.87\ m_\pi^{-1}$. The analysis is shown in Fig. 2. In the left panel, the doublet $n$-$d$ scattering length, ${}^2a_{nd}$, is given as a function of the parameter $b$ (in units of its original value, $b_0 = -2.58\ m_\pi^{-3}$) for different values of the cutoff $\Lambda$ (in units of $m_\pi$). The box at the top of the figure includes those values of ${}^2a_{nd}$ compatible with the experimental results. At each point of the curves, the value of the constant $d$ has been varied to reproduce the triton binding energy. Its corresponding values (in units of its original value, $d_0 = -0.753\ m_\pi^{-3}$) are given as a function of $b$ in the right panel in Fig. 2. Therefore, each point in the curves in both panels corresponds to a set of parameters that, in connection with the AV18 potential, reproduces the triton binding energy. The variations of the parameters given in Fig. 2 do not exhaust all the possibilities. The analysis was done maintaining the attractive character of the $b$ and $d$ terms, and therefore, the lines in the left panel stop when one of the two parameters, $b$ or $d$, changes sign. We can see that, with the AV18 + TM′ potential, there is a very small region in the parameters' phase space available for a simultaneous description of the triton binding energy and the doublet scattering length. This small region corresponds to a value of $b$ about four times larger than the original value $b_0$, and $d$ turns out to be almost zero. Moreover, the value of the cutoff $\Lambda$ around $3.8\ m_\pi$ is smaller than the values usually used with the TM′ potential ($\Lambda \approx 5\ m_\pi$).

Note that, for negative values of the parameters $a$, $b$, and $d$, the TM′ potential is attractive and it does not include explicitly a repulsive term. Added to a specific $NN$ potential that underestimates the three-nucleon binding energy, it supplies the extra binding by fixing its strength appropriately. As mentioned in Sec. I, the scattering length is sensitive to the balance between the attractive part and the repulsive part of the complete interaction. Therefore, in the case of the TM′ potential, it seems that by introducing only attractive terms,

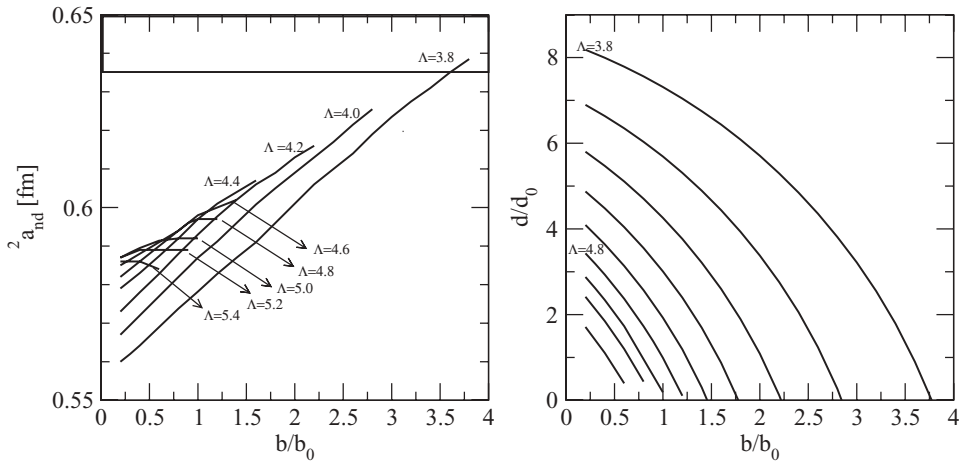


FIG. 2. Doublet scattering length ${}^2a_{nd}$ as a function of parameter $b$ (in units of the original parameter, $b_0 = -2.58\ m_\pi^{-3}$) of the TM′ potential for different values of the cutoff and corresponding values of parameter $d$ (in units of the original parameter, $d_0 = -0.753\ m_\pi^{-3}$), as a function of parameter $b$, used to reproduce the triton binding energy.

fixed to reproduce the triton binding energy, it is difficult to reproduce correctly this balance.

As discussed before, the TM′ potential is a modification of the original TM potential compatible with chiral symmetry. At next-to-next-to-leading order in the chiral effective field theory, the $D$ and $E$ terms appear (see Ref. [9], and references therein) as given in Eq. (2). Here we introduce the following additional term to the TM′ potential, based on a contact term of three nucleons:

$$W_E^{\rm TM}(1,2,3) = W_0^E \; Z_0^{\rm TM}(r_{31}) Z_0^{\rm TM}(r_{23}). \qquad (14)$$

This term corresponds to the $E$ term in Eq. (2), except that, for the sake of simplicity, we have omitted the $(\boldsymbol{\tau}_1 \cdot \boldsymbol{\tau}_2)$ operator. Its strength $W_0^E$ is defined in Eq. (12), and the function $Z_0^{\rm TM}$, defined in Eq. (13), is a positive function; therefore, for positive values of $c_E$, the new term is repulsive. We include it in the following analysis of the TM′ potential. The results are shown in Fig. 3 for three values of $\Lambda/m_\pi$: 4, 4.8, and 5.6. In the left panels the doublet $n$-$d$ scattering length is given as a function of the parameter $b$ (in units of $b_0$) for different values of the strength $c_E$ of the $E$ term. The bold boxes include those values compatible with the experimental results. At each point on the curves, the value of the constant $d$ has been varied to reproduce the triton binding energy. For selected values of the parameters inside the box, the predictions for the $^4$He binding energy $B(^4\text{He})$ are shown in the right panels.

Comparing the left panels in Figs. 2 and 3, the effect of the new term is clear. In Fig. 2 we observed that using $\Lambda \geqslant 4\, m_\pi$, ${}^2a_{nd}$ cannot be well reproduced. Conversely, in Fig. 3, the inclusion of the new term allows for the description of ${}^2a_{nd}$ using different values of the cutoff. The values of the parameter $b$ are closer to its original value as $\Lambda$ increases. Opposite to this, the predictions of $B(^4\text{He})$ improve as $\Lambda$ decreases. For example, considering the case $\Lambda = 4\, m_\pi$, ${}^2a_{nd}$, $B(^3\text{H})$ and $B(^4\text{He})$ are well reproduced with $b = 3.2 b_0$, $d = 6.2 d_0$, and $c_E = 1$. With $\Lambda = 4.8\, m_\pi$ the set of parameters that gives the best description of the three quantities is $b = 1.5 b_0, d = 4.5 d_0$, and $c_E = 1.6$. And with $\Lambda = 5.6\, m_\pi$ they are $b = 0.8 b_0$, $d = 3 d_0$, and $c_E = 2$. Their different contributions to the triton binding energy are given in Table II, where we report the mean values of the kinetic energy and the $NN$ potential energy as well as the mean values of the attractive part of the TNF, $V_A(3N)$, corresponding to the sum of the $a$, $b$, and $d$ terms, and the repulsive part, $V_R(3N)$, corresponding to the $c_E$ term. The last two columns in Table II list the $B(^4\text{He})$ and ${}^2a_{nd}$ values. For the sake of comparison, in the first row, the original values of the parameters were considered ($b = b_0$, $d = d_0$, and $c_E = 0$) with the value of the cutoff fixed to reproduce the triton binding energy ($\Lambda = 4.8\, m_\pi$). As we can see, in this case $B(^4\text{He})$ is overestimated and ${}^2a_{nd}$ is underestimated. When the $E$ term is considered, the description of $B(^4\text{He})$ improves and it seems that a low value of $\Lambda$ is preferable. Further analysis of these parametrizations is given in Sec. IV, studying some polarization observables at low energy.

### B. Urbana IX force

In the following we analyze the URIX potential, which has two parameters, called $A_{2\pi}^{\rm PW}$ and $A_R$. In this model the strength of the $d$ term is related to the strength of the $b$ term as $d = b/4$. The original values of the parameters were fixed in Ref. [3] in conjunction with the AV18 $NN$ potential, and from Table I, we observe that the model correctly describes the triton binding energy. However, it overestimates $B(^4\text{He})$ and underestimates ${}^2a_{nd}$. To further analyze the origin of this behavior, we have varied the constants $A_{2\pi}^{\rm PW}$ and $A_R$ and the relative strength $D_{2\pi}^{\rm PW} = d/b$ of the $b$- and $d$-terms. The regularization parameter has been held fixed at its original value, $c = 2.1\ \text{fm}^{-2}$. For a given value of $A_{2\pi}^{\rm PW}$, the values of $A_R$ and $D_{2\pi}^{\rm PW}$ have been chosen to reproduce $B(^3\text{H})$ and ${}^2a_{nd}$. The results are shown in Fig. 4. In Fig. 4(a), $D_{2\pi}^{\rm PW}$ is given as a function of $A_{2\pi}^{\rm PW}$, with $A_R$ varying from 0.0176 MeV at $A_{2\pi}^{\rm PW} = -0.02$ to 0.0210 MeV at $A_{2\pi}^{\rm PW} = -0.050$ MeV. These values of $A_R$ are more than three times larger than the original value of 0.0048 MeV. Figures 4(b) and 4(c), respectively, give the results for ${}^2a_{nd}$ and $B(^4\text{He})$. The latter was not included in the determination of the parameters, as $D_{2\pi}^{\rm PW}$ and $A_R$ were determined from the triton binding energy and ${}^2a_{nd}$ and are, therefore, pure predictions. We observe a slight overestimation of $B(^4\text{He})$, in particular, for values of $|A_{2\pi}^{\rm PW}| > 0.04$ MeV, corresponding to values of $D_{2\pi}^{\rm PW} < 0.7$.

With modifications of the parameters in the URIX force, we were able to describe $B(^3\text{H})$, ${}^2a_{nd}$ and $B(^4\text{He})$ reasonably well. However, this was achieved with a substantial increase in the repulsive term. To gain insight into the consequence of the new parametrizations in the quantities of interest, in Table III we report the mean values of the kinetic energy and the $NN$ potential energy as well as the mean values of the attractive part of the TNF, $V_A(3N)$, corresponding to the sum of the $b$ and $d$ terms, and the repulsive part, $V_R(3N)$, corresponding to the $A_R$ term, for selected values of the parameters (indicated by circles in Fig. 4). The last two columns in Table III show $B(^4\text{He})$ and ${}^2a_{nd}$. For the sake of comparison, in the first row, the values obtained using the original AV18 + URIX model are reported. From the table we observe that some of the values considered for $D_{2\pi}^{\rm PW}$ and $A_R$ are quite far from the original ones. At the original value of $A_{2\pi}^{\rm PW}$, $-0.0293$ MeV, the relative strength now results to be $D_{2\pi}^{\rm PW} = 1$ and $A_R = 0.0181$ MeV. As $D_{2\pi}^{\rm PW}$ diminishes, $A_R$ tends to increase further, with the consequence that the mean value $V_R(3N)$ is more than three times larger than the value obtained using the original parameters (listed in the first row in Table III). This is compensated by a lower mean value of the kinetic energy. Further analysis of the effects of the parametrizations given in Table III is reported in Sec. IV, studying selected $p$-$d$ polarization observables.

### C. N2LOL force

The parameters $c_1$, $c_3$, and $c_4$ of the N2LOL model were taken from the the chiral N3LO $NN$ force in Ref. [15], whereas the $c_D$ and $c_E$ parameters were determined in Ref. [10], in conjunction with that $NN$ force, by fitting $B(^3\text{H})$ and $B(^4\text{He})$. Here we use the N2LOL force in conjunction with the AV18 $NN$ interaction, so we have to modify its parametrization because the amount of attraction to be gained is now different (see Table I). In the following we call $c_1^0$, $c_3^0$, and $c_4^0$ the values of these constants, given in Sec. II, determined in Ref. [15]. Among the different possibilities, in Fig. 5 we show

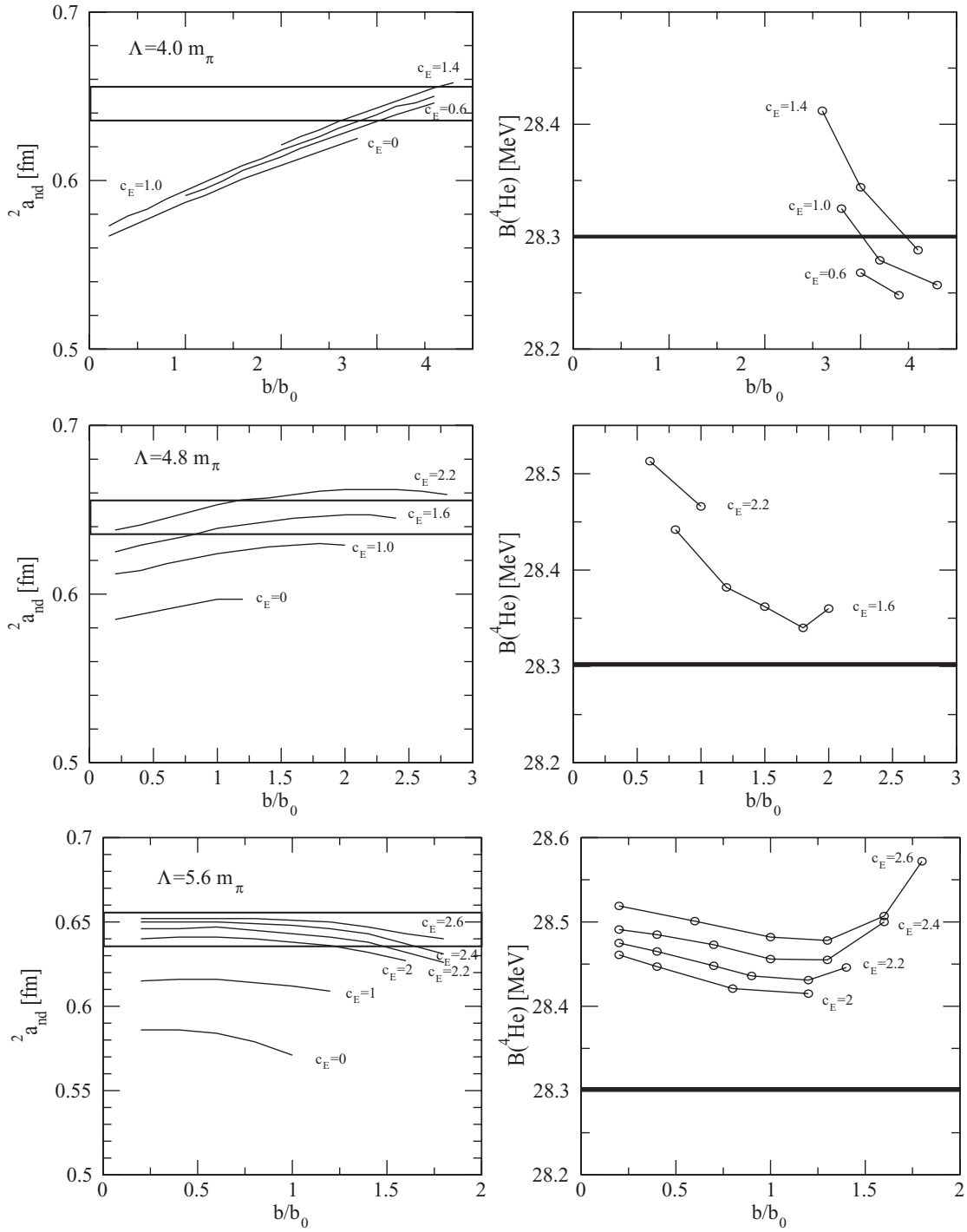


FIG. 3. Doublet scattering length $a_{nd}$ as a function of parameter $b$ (in units of $b_0 = -2.58\ m_\pi^{-3}$) of the TM′ potential including the $W_E^{\rm TM}$ term, for different values of the strength $c_E$ and for three selected values of $\Lambda$. Corresponding values of $B(^4\mathrm{He})$, for specific values of $a_{nd}$ inside the bold box, are shown in the right panels (circles).

a new parametrization of the N2LOL interaction, obtained by multiplying $c_3^0$ and $c_4^0$ by a factor $c_0$ and maintaining $c_1 = c_1^0$. Then the parameters $c_D$ and $c_E$ were determined from a fit to $B(^3\mathrm{H})$ and $^2a_{nd}$. They are shown as a function of $c_0$ in Fig. 5(a). Therefore, at a fixed value of $c_0$, with the set of parameters $c_1 = c_1^0$, $c_3 = c_0 c_3^0$, $c_4 = c_0 c_4^0$ and the corresponding values of $c_D$ and $c_E$ extracted from the figure, the AV18 + N2LOL interaction reproduces the $B(^3\mathrm{H})$ and $^2a_{nd}$. In Fig. 5(b) we show the stability obtained in the description of the doublet scattering length corresponding to the constant value chosen for the determination of the parameters, $^2a_{nd} = 0.644$ fm. With the new set of parameters it is now possible to calculate $B(^4\mathrm{He})$. This is shown in Fig. 5(c), and it is interesting to note that in all cases the value $B(^4\mathrm{He}) = 28.60$ MeV was obtained.

TABLE II. Mean values of the triton kinetic energy and the two-nucleon potential energy $V(2N)$, and the attractive, $V_A(3N)$, and repulsive, $V_R(3N)$, contributions of the TNF to the triton binding energy using the AV18 + TM′ potential for the specified values of the parameters and with $a = -0.87\ m_\pi^{-1}$. $B(^4\mathrm{He})$ and $^2a_{nd}$ are given in the last two columns. Experimental values are given in the last row.

| $b\ (m_\pi^{-3})$ | $d\ (m_\pi^{-3})$ | $c_E$ | $\Lambda\ (m_\pi)$ | $T$ (MeV) | $V(2N)$ (MeV) | $V_A(3N)$ (MeV) | $V_R(3N)$ (MeV) | $B(^4\mathrm{He})$ (MeV) | $^2a_{nd}$ (fm) |
|---|---|---|---|---|---|---|---|---|---|
| −2.580 | −0.753 | 0.0 | 4.8 | 50.708 | −58.144 | −1.039 | 0.0 | 28.52 | 0.596 |
| −8.256 | −4.690 | 1.0 | 4.0 | 50.317 | −57.366 | −2.206 | 0.781 | 28.30 | 0.644 |
| −3.870 | −3.375 | 1.6 | 4.8 | 50.699 | −57.641 | −2.748 | 1.215 | 28.38 | 0.644 |
| −2.064 | −2.279 | 2.0 | 5.6 | 50.998 | −57.940 | −2.814 | 1.291 | 28.44 | 0.640 |
| Exp. | | | | | | | | 28.30 | $0.645 \pm 0.003 \pm 0.007$ |

Also, with modification of the parameter $c_1$ to $c_1 = c_0 c_1^0$, slightly different values of $c_D$ and $c_E$ are obtained. Using these values to calculate $B(^4\mathrm{He})$, again we obtain a constant value, which is now = 28.55 MeV. Similar analyses using slightly different values of the cutoff $\Lambda$ around 500 MeV did not show to change these results.

To correctly describe $B(^4\mathrm{He})$, after fixing $B(^3\mathrm{H})$ and $^2a_{nd}$, we now analyze a modification of the relative strength of the $b$ and $d$ terms that, in the previous analysis, was maintained at its original value of $c_4^0/c_3^0 = 1.6875$. To this end we performed a study similar to those done previously for the other TNF models. Fixing the constant $c_1$ to its original value $c_1^0$, $c_3$, $c_4$, $c_D$, and $c_E$ were varied. The analysis is shown in Fig. 6 at $c_E$ values of 0, 0.1, −0.03, and −0.5 and for the indicated values of $c_D$ chosen to reproduce $^2a_{nd}$ (left panels). The predictions for $B(^4\mathrm{He})$ are given in the right panels for those values of the parameters that give a value of $^2a_{nd}$ inside the bold box. At each point in the curves in the left and the right panels, $c_4$ was chosen to reproduce the triton binding energy. Owing to the $(\boldsymbol{\tau}_i \cdot \boldsymbol{\tau}_j)$ operator in the $E$ term of the N2LOL potential, positive values of $c_E$ makes this term attractive. Conversely, negative values of $c_E$ make this term repulsive. We considered only one positive case, $c_E = 0.1$. Increasing $c_E$ further, we found it difficult to describe $B(^4\mathrm{He})$ correctly. For negatives values of $c_E$ we considered two cases: $c_E = -0.03$, which corresponds to the value given in Ref. [10], and $c_E = -0.5$. In Fig. 6 we observe an almost-linear behavior of $^2a_{nd}$. There is a slight curvature for negative values of $c_D$ in the upper three panels. The analysis of $B(^4\mathrm{He})$ selects the values of $c_D$. We found that the experimental value was well reproduced for the pairs $(c_D = -0.5, c_E = 0.1)$, $(c_D = -1, c_E = 0)$, $(c_D = -1, c_E = -0.03)$, and $(c_D = -2, c_E = -0.5)$.

In Table IV we report the mean values of the kinetic energy and the two-nucleon potential energy—as well as the mean values of the attractive part of the TNF, $V_A(3N)$, and its repulsive part, $V_R(3N)$—for the selected values of the parameters that correspond to the best description of the three quantities under study. $B(^4\mathrm{He})$ and $^2a_{nd}$ are listed in the last two columns in Table IV. The contributions to $V_A(3N)$ come from the $a$, $b$, $d$, and $D$ terms, which are always attractive in the cases considered, and from the $E$ term in the first case. This term contributes to the repulsive part $V_R(3N)$ in the latter two cases. From Table IV we can observe that $c_3$ and $c_4$ turn out to be larger and smaller than their original values, respectively. This is a consequence of the simultaneous description of $B(^3\mathrm{H})$ and $^2a_{nd}$. Furthermore, in the first three cases, the ratio $c_4/c_3 \approx 0.46$, is much lower than the original ratio.

## IV. ANALYSIS OF THE POLARIZATION OBSERVABLES

In the previous section we studied different parametrizations of the TM′, URIX, and N2LOL TNF models in conjunction with the AV18 NN potential. The analysis was done by first varying the parameters to reproduce $B(^3\mathrm{H})$ and then looking at their dependence on $^2a_{nd}$ and $B(^4\mathrm{He})$. To improve the description of these quantities, some substantial modifications were necessary for the first two models. In the case of the TM′ interaction we found the inclusion of a repulsive term to be opportune. In the analysis of the URIX interaction, the strength

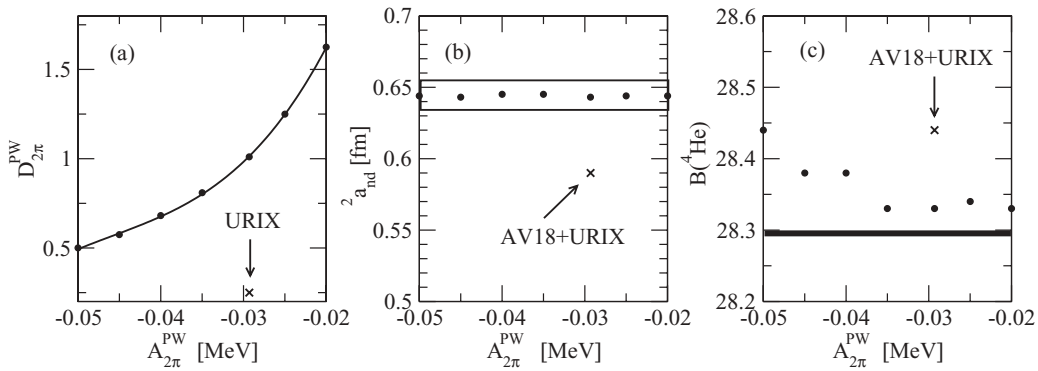


FIG. 4. (a) Relative strength $D_{2\pi}^{PW}$, (b) $^2a_{nd}$, and (c) $B(^4\mathrm{He})$ as functions of $A_{2\pi}^{PW}$, for the AV18 + URIX model.

TABLE III. Mean values of the triton kinetic energy, the two-nucleon potential energy $V(2N)$, and the attractive, $V_A(3N)$, and repulsive, $V_R(3N)$, contributions of the TNF to the triton binding energy using the AV18 + URIX potential for the specified values of the parameters. $B(^4\mathrm{He})$ and $^2a_{nd}$ are given in the last two columns, respectively. Experimental values are listed in the last row.

| $A_{2\pi}^{\mathrm{PW}}$ (MeV) | $D_{2\pi}^{\mathrm{PW}}$ | $A_R$ (MeV) | $T$ (MeV) | $V(2N)$ (MeV) | $V_A(3N)$ (MeV) | $V_R(3N)$ (MeV) | $B(^4\mathrm{He})$ (MeV) | $^2a_{nd}$ (fm) |
|---|---|---|---|---|---|---|---|---|
| −0.0293 | 0.25 | 0.0048 | 51.259 | −58.606 | −1.126 | 1.000 | 28.48 | 0.578 |
| −0.0200 | 1.625 | 0.0176 | 47.472 | −57.976 | −0.923 | 2.950 | 28.33 | 0.644 |
| −0.0250 | 1.25 | 0.0182 | 47.628 | −57.967 | −1.162 | 3.024 | 28.34 | 0.644 |
| −0.0293 | 1.00 | 0.0181 | 47.876 | −58.000 | −1.369 | 3.015 | 28.33 | 0.643 |
| −0.0350 | 0.8125 | 0.0191 | 47.998 | −57.975 | −1.649 | 3.147 | 28.33 | 0.645 |
| −0.0400 | 0.6875 | 0.0198 | 48.133 | −57.964 | −1.897 | 3.249 | 28.38 | 0.645 |
| −0.0450 | 0.5625 | 0.0198 | 48.414 | −57.995 | −2.148 | 3.248 | 28.38 | 0.643 |
| −0.0500 | 0.50 | 0.0210 | 48.471 | −57.952 | −2.401 | 3.401 | 28.44 | 0.645 |
| Exp. | | | | | | | 28.30 | $0.645 \pm 0.003 \pm 0.007$ |

of the repulsive term proved to be more than three times larger than the original value, and the relative strength of the $b$ and $d$ terms, originally fixed at 1/4, also increased. In the case of the N2LOL interaction, some adjustment of the parameters was necessary, mainly owing to the fact that the AV18 interaction is less attractive than the N3LO interaction, from which the N2LOL model was originally parametrized. In this section we analyze the effects of the new parametrizations in observables that are not correlated with the binding energies or with $^2a_{nd}$. Some polarization observables in $p$-$d$ scattering have this characteristic, in particular, the vector and tensor analyzing powers. In Figs. 7, 8, and 9 we show the differential cross section $d\sigma/d\Omega$, the vector polarization observables $A_y$ and $iT_{11}$, and the tensor polarization observables $T_{20}$, $T_{21}$, and $T_{22}$ at $E_{\mathrm{lab}} = 3$ MeV for the different potential models compared to the results obtained using the original AV18 + URIX interaction. In the figures, the lighter, shaded (cyan) band represents the results obtained with the parameters given in the last three rows in Table II, the second to the sixth rows in Table III, and the last three rows in Table IV for each model, respectively, whereas the solid line is the prediction of the original AV18 + URIX model. As we can see, for each TNF model, the observables calculated using the different parametrizations, fixed from a simultaneous description of $B(^3\mathrm{H})$, $^2a_{nd}$, and $B(^4\mathrm{He})$, fall in bands that, in the case of the vector analyzing powers, have different positions for the three models. Because the models essentially differ in the definitions of the functions $y(r)$, $T(r)$, and $Z_0(r)$, this difference can be associated with the different short-range behavior of the TNF models. Figure 7 shows that the AV18 + TM′ model, using the new parametrizations, does not give any improvement in the observables compared to the AV18 + URIX predictions. Moreover, $iT_{11}$ and $T_{21}$ are not described as well. It should be noted that the AV18 + TM′ model, with the original parametrization, and the AV18 + URIX give similar results for the observables (a small difference can be observed in the maximum of $A_y$, being slightly higher for the former). Therefore the previous conclusions do not change compared to the original AV18 + TM′ model. Figure 8 shows that the new parametrizations of the AV18 + URIX model produce much worse descriptions of $A_y$, $iT_{11}$, and $T_{21}$. Because the vector analyzing powers are mainly described by the $P$-wave phase-shift and mixing parameters, we can conclude that they are poorly reproduced with the new parametrizations. Conversely to the results of the analyses of the previous models, Fig. 9 shows that the N2LOL interaction produces an improvement in the description of $A_y$ and $iT_{11}$. The well-known discrepancy in these observables is now reduced, and for $A_y$, in particular, the improvement is noticeable. In the case of the tensor analyzing powers, a slightly worse description of $T_{21}$ between the two

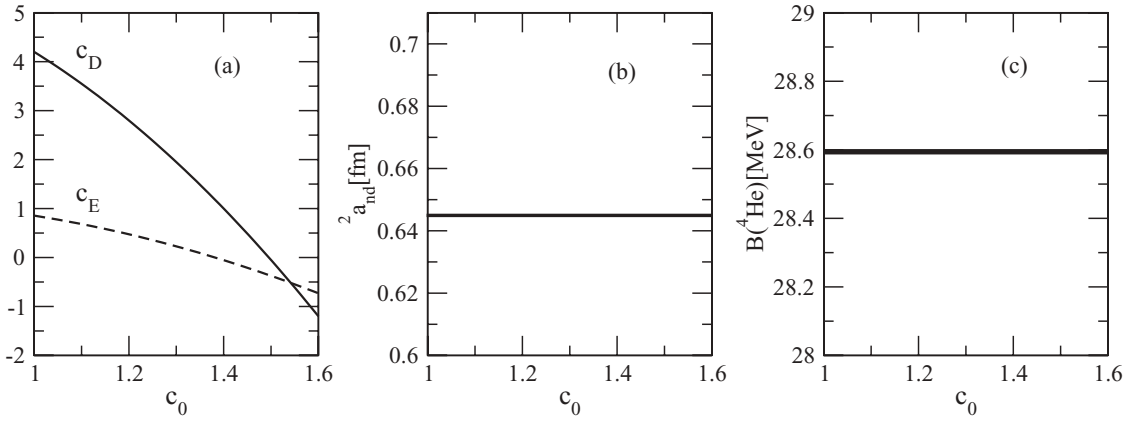


FIG. 5. (a) $c_D$ and $c_E$ parameters, (b) $^2a_{nd}$, and (c) $B(^4\mathrm{He})$, as functions of $c_0$, for the AV18 + N2LOL model.

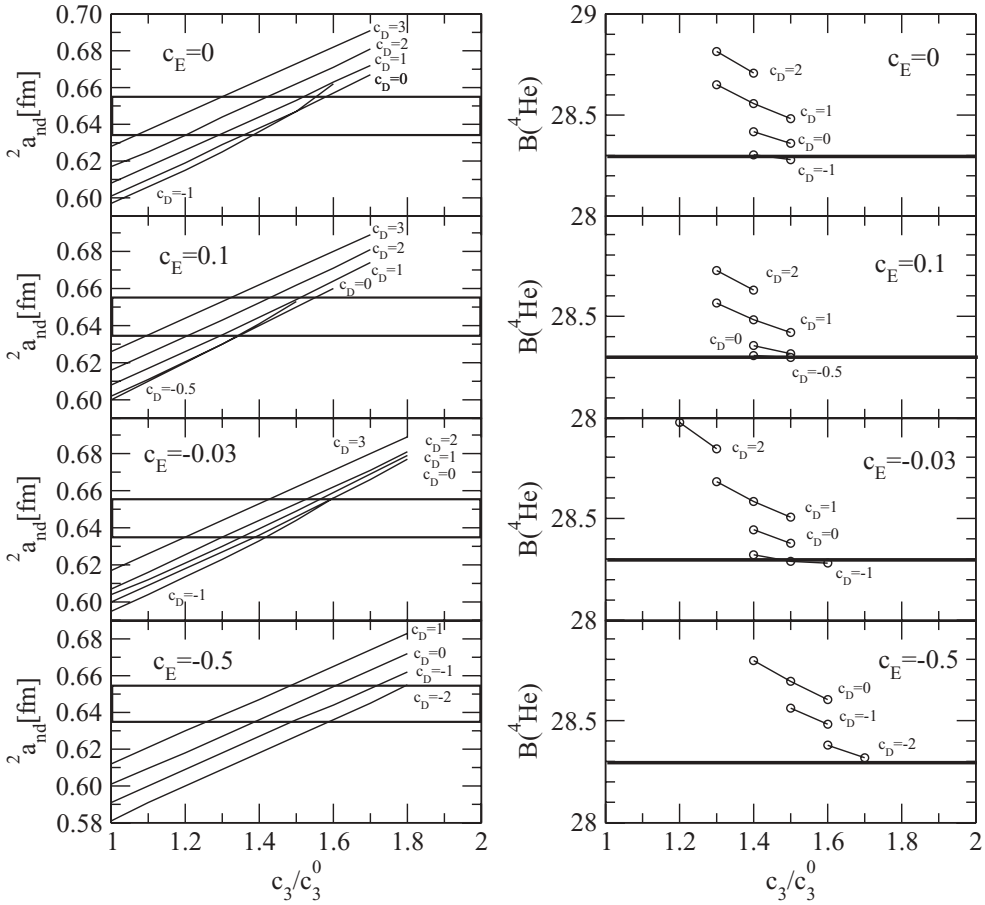


FIG. 6. Doublet scattering length ${}^2a_{nd}$ as a function of parameter $c_3$ (in units of $c_3^0 = -0.0032\,\mathrm{MeV}^{-1}$) of the N2LOL potential, for different values of the strength $c_D$, at four selected values of $c_E$. Corresponding values of $B({}^4\mathrm{He})$, for specific values of $a_{nd}$ inside the bold box, are shown in the right panels (circles).

maxima is now observed. In general all TNFs of the type analyzed here have this effect in $T_{21}$, indicating that a different mechanism, not present in the models, should be considered to improve the description of the minimum around 75°.

Finally, we would like to comment on the fact that the vector analyzing powers, $A_y$ and $iT_{11}$, calculated using different TNF models fall inside a band with a different position for each model. In Fig. 10 the three bands extracted from Figs. 7–9 are shown explicitly and compared to the original AV18 + URIX model (solid line). We can clearly see the different positions of the bands, with the best description obtained with the new parametrizations of the AV18 + N2LO model and the worst description with those of the AV18 + URIX model. Because all the models within the bands describe $B({}^3\mathrm{H})$, ${}^2a_{nd}$, and $B({}^4\mathrm{He})$ reasonably well, we can conclude that the difference is a direct consequence of their different short-range structures. A natural question is whether, with opportune modifications of their radial dependence, that is, modifications of the functions $y(r)$, $T(r)$, and $Z_0(r)$, it will be possible to improve further the description of these observables at $E_{\mathrm{lab}} = 3\,\mathrm{MeV}$ and, eventually, obtain a $\chi^2$ per datum close to 1. A preliminary study in this direction has shown that a further improvement

TABLE IV. Mean values of the triton kinetic energy, the two-nucleon potential energy $V(2N)$, and the attractive, $V_A(3N)$, and repulsive, $V_R(3N)$, TNF contributions to the triton potential energy using the AV18 + N2LOL potential for the specified values of the parameters and with $c_1 = -0.00081\,\mathrm{MeV}^{-1}$. $B({}^4\mathrm{He})$ and ${}^2a_{nd}$ are given in the last two columns. Experimental values are listed in the last row.

| $c_3$ ($c_3^0$) | $c_4$ ($c_4^0$) | $c_D$ | $c_E$ | $T$ (MeV) | $V(2N)$ (MeV) | $V_A(3N)$ (MeV) | $V_R(3N)$ (MeV) | $B({}^4\mathrm{He})$ (MeV) | ${}^2a_{nd}$ (fm) |
|---|---|---|---|---|---|---|---|---|---|
| 1.4 | 0.3636 | −0.5 | 0.1 | 49.834 | −57.278 | −1.029 | 0.0 | 28.31 | 0.641 |
| 1.4 | 0.3786 | −1 | 0.0 | 49.950 | −57.401 | −1.022 | 0.0 | 28.30 | 0.636 |
| 1.5 | 0.3735 | −1 | −0.03 | 49.839 | −57.274 | −1.076 | 0.036 | 28.29 | 0.644 |
| 1.7 | 0.9000 | −2 | −0.50 | 50.166 | −57.181 | −2.119 | 0.657 | 28.32 | 0.645 |
| Exp. | | | | | | | | 28.30 | $0.645 \pm 0.003 \pm 0.007$ |

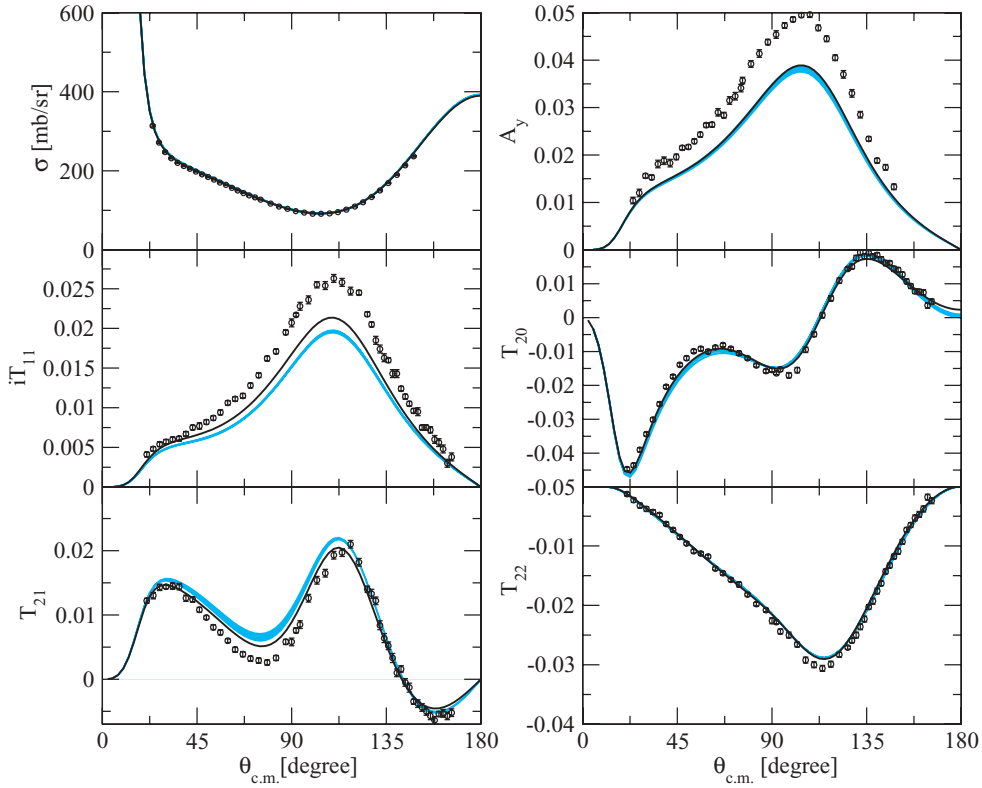


FIG. 7. (Color online) Differential cross section and vector and tensor polarization observables at $E_{\rm lab} = 3$ MeV using the AV18 + TM′ model with the parameters listed in the last three rows in Table II [lighter, shaded (cyan) band]. The predictions of the AV18 + URIX model (solid line) and the experimental points from Ref. [25] are also shown.

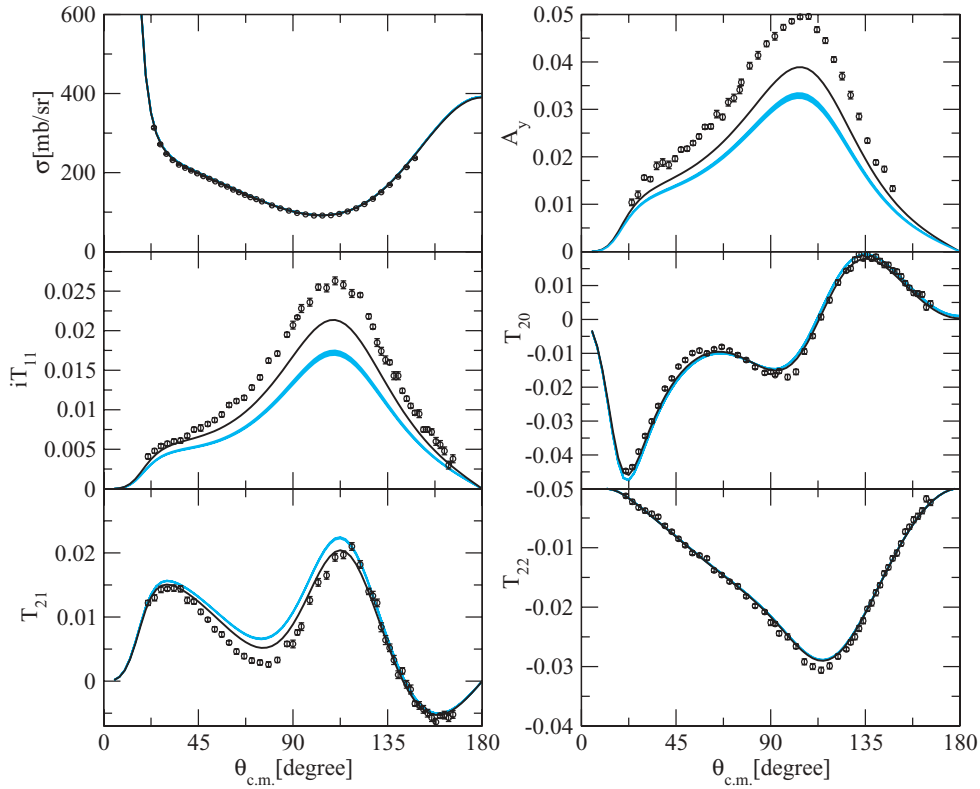


FIG. 8. (Color online) Differential cross section and vector and tensor polarization observables at $E_{\rm lab} = 3$ MeV using the AV18 + URIX model with the parameters given in Table III [lighter, shaded (cyan) band]. The predictions of the original AV18 + URIX model, given in the first row of the table, are shown as a solid line. The experimental points from Ref. [25] are also shown.

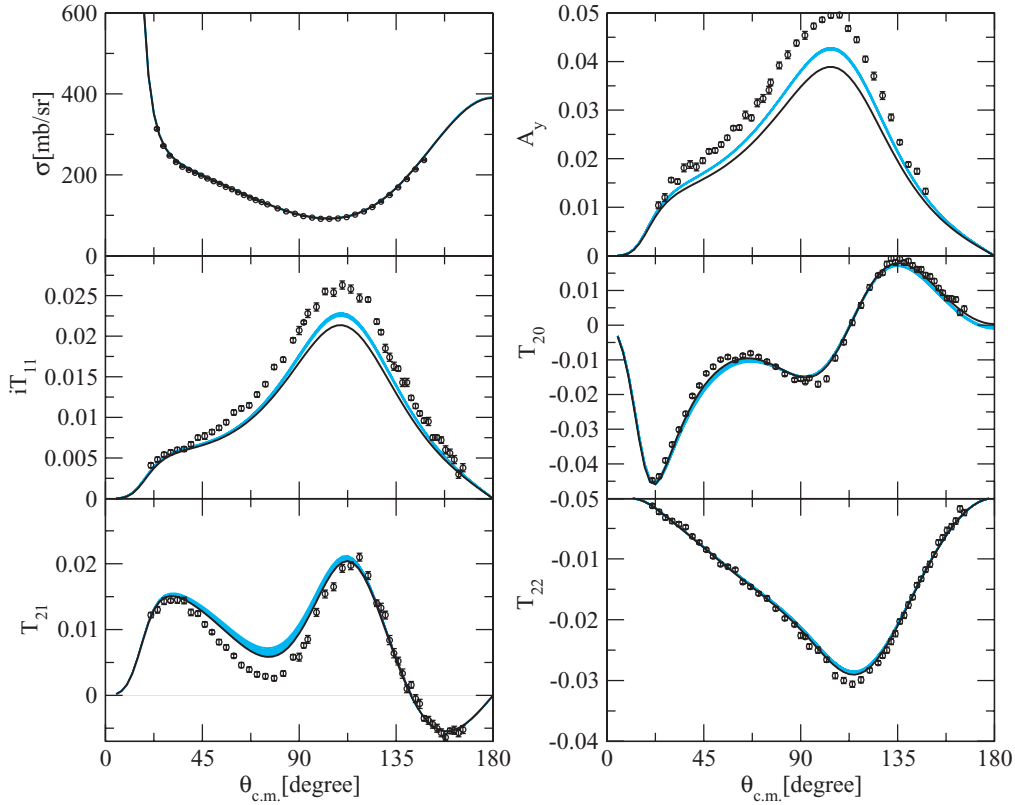


FIG. 9. (Color online) Differential cross section and vector and tensor polarization observables at $E_{\rm lab} = 3$ MeV using the AV18 + N2LOL model with the parameters given in Table IV [lighter, shaded (cyan) band]. The predictions of the AV18 + URIX model (solid line) and the experimental points from Ref. [25] are also shown.

in the $A_y$ and $iT_{11}$ maxima is associated with a worse description of the $T_{21}$ minimum. The particular structure of these observables is related to a bigger splitting in the $^4P_J$ phase shifts than the normal splitting produced by the two-nucleon forces, as discussed in Ref. [26]. In particular, the $^4P_{1/2}$ phase shift has to be smaller and the mixing parameter $\epsilon_{3/2-}$ has to be bigger. It is a general feature of the TNFs studied here that both, $^4P_{1/2}$ and $\epsilon_{3/2-}$ tend to increase. To be more precise, Table V show the $^4P_J$ phase shifts and $\epsilon_{3/2-}$ for the AV18 and AV18 + URIX potential models and for one selected set of the parameters in Tables II, III, and IV, corresponding to the new parametrizations of the AV18 + TM′, AV18 + URIX, and AV18 + N2LOL models (indicated in the table by an asterisk). In particular, parametrizations in the second row in Table II, the fourth row in Table III, and the third row in Table IV were used, respectively. In the last row in Table V, results from the phase-shift analysis in Ref. [26] are reported. Table V shows that the $^4P_{1/2}$ phase shift increases when the TNF models are added to the AV18 potential. By itself, this change will produce a much worse description of $A_y$ and $iT_{11}$. However, this is well compensated by the corresponding increase in $^4P_{5/2}$ and $\epsilon_{3/2-}$. This is not the case for the minimum in $T_{21}$, for which a better description would be obtained by lowering the AV18 value of $^4P_{1/2}$, as discussed in Ref. [26]. The other parametrizations listed in Tables II, III, and IV produce similar changes in the $^4P_J$ parameters. From this

TABLE V. $^4P_J$ phase shifts and the $\epsilon_{3/2-}$ mixing parameter at $E_{\rm lab} = 3$ MeV for the potential models indicated. For sake of comparison, results of the phase-shift analysis (PSA) from Ref. [26] are listed in the last row.

| | $^4P_{1/2}$ | $^4P_{3/2}$ | $^4P_{5/2}$ | $\epsilon_{3/2-}$ |
|---|---|---|---|---|
| AV18 | 22.03 | 24.24 | 24.08 | −2.247 |
| AV18 + URIX | 22.31 | 24.30 | 24.27 | −2.314 |
| AV18 + TM′* | 22.79 | 24.45 | 24.53 | −2.453 |
| AV18 + URIX* | 22.75 | 24.41 | 24.35 | −2.375 |
| AV18 + N2LOL* | 22.55 | 24.25 | 24.48 | −2.394 |
| PSA | 21.77 ± 0.01 | 24.30 ± 0.01 | 24.26 ± 0.01 | −2.46 ± 0.01 |

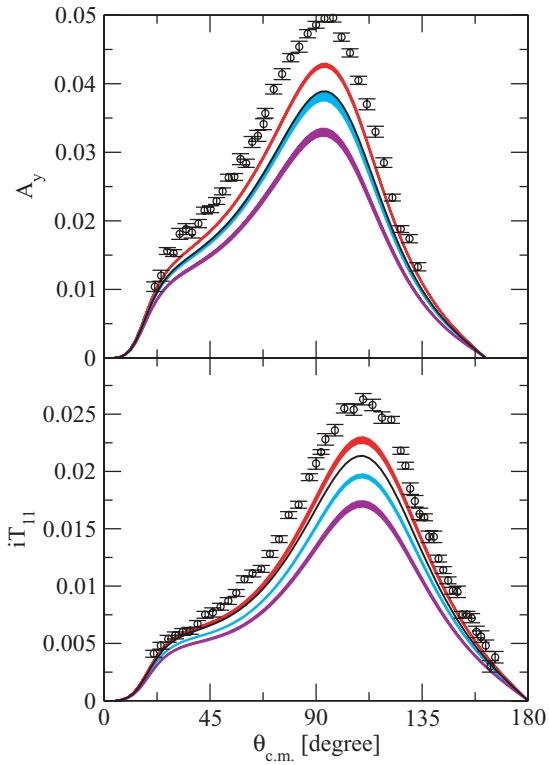


FIG. 10. (Color online) The vector analyzing powers $A_y$ and $iT_{11}$ at $E_{lab} = 3$ MeV using the AV18 + TM′ [third from bottom (cyan) band], AV18 + URIX [bottom (violet) band], and AV18 + N2LOL [top (red) band] models as in Figs. 7, 8, and 9. The predictions of the AV18 + URIX model (solid line) and the experimental points from Ref. [25] are also shown.

observation we can conclude that the spin-isospin structure of the TNFs considered here is not sufficient to describe $B(^3\mathrm{H})$, $^2a_{nd}$, and $B(^4\mathrm{He})$ simultaneously or the vector and tensor analyzing powers at low energies.

## V. CONCLUSIONS

Stimulated by the fact that some of the widely used TNF models do not reproduce simultaneously the triton and the $^4$He binding energies and the $n$-$d$ doublet scattering length, we have analyzed possible modifications of their parametrizations. To this end, we selected the AV18 as the reference two-nucleon force, and associated with it, we varied the original parameters of the TM′ and URIX models so as to improve the description of the three quantities mentioned. Furthermore, using the recent local form of a chiral TNF (we call this model N2LOL), we have also studied its parametrization associated with the AV18 interaction. The analysis proceeded in the following way. The three models under examination, TM′, AV18, and N2LOL, were written in configuration space as a sum of five terms: $a$, $b$, $d$, $C$, and $E$. The first three, corresponding to a two-pion exchange process, are attractive. The last two, corresponding to contact terms, can be either attractive or repulsive. Not all the models include the five terms. In the TM′ model, only the $a$, $b$, and $d$ terms are present, and therefore this model does not include explicitly a repulsive term. The URIX model includes the $b$, $d$, and $E$ terms. The latter term has been parametrized as repulsive to compensate the large overbinding produced by the first two terms in infinite nuclear matter. The N2LOL model includes the five terms.

The study includes analysis of the AV18 + TM′ model. Maintaining the strength of the $a$ term fixed at its original value, we have varied the strengths of the $b$ and $d$ terms for several values of the cutoff parameter $\Lambda$. We have explored negative values of the strength parameters $b$ and $d$, to keep the attractive character of these terms. We found it difficult to reproduce $^2a_{nd}$ for reasonable values of the strength parameters. This fact motivated the subsequent step of introducing a repulsive term in the model. As a simple choice, we have introduced a purely central $E$ term and a corresponding $Z_0(r)$ function, obtained using the monopole cutoff of the model. By including this term we were able to describe $B(^3\mathrm{H})$ and $^2a_{nd}$ simultaneously for several values of the cutoff. Further selection among these values was done from the calculation of $B(^4\mathrm{He})$. We observed that with $\Lambda \leqslant 4.8\, m_\pi$ it is possible to describe the three quantities reasonably well.

In the original AV18 + URIX model the relative strength between the $b$ and the $d$ terms was fixed. In the present analysis we have relaxed this condition, increasing the number of parameters in the model from two to three, the strengths of the $b$, $d$, and $E$ terms. By varying them, we have found it possible to describe the three quantities of interest for values of the parameters very different from their original ones. In particular, the strength of the repulsive term proved to be more than three times larger than the original value. In the case of the AV18 + N2LOL model, maintaining the strength of the $a$ term fixed at its original value, we varied the parameters $c_3$, $c_4$, $c_D$, and $c_E$ in combinations that reproduce $B(^3\mathrm{H})$. Then we studied the dependence on $^2a_{nd}$ and $B(^4\mathrm{He})$ of the different parametrizations. For fixed values of $c_E$ we have calculated $^2a_{nd}$ for different values of $c_3$ and $c_D$. We have found that $c_3 \geqslant 1.4c_3^0$ to describe $B(^3\mathrm{H})$ and $^2a_{nd}$ simultaneously. Values of $c_D$ have been selected from the analysis of $B(^4\mathrm{He})$. Values of $B(^4\mathrm{He})$ compatible with the experimental value were found in the four cases of $c_E$ explored.

After completing this sensitivity study we have selected, for each model, some combinations of the parameters that give better descriptions of $B(^3\mathrm{H})$, $^2a_{nd}$, and $B(^4\mathrm{He})$ and we have calculated the differential cross section and the vector and tensor analyzing powers at $E_{lab} = 3$ MeV. At this energy there are well-established discrepancies between the predictions of the theoretical models and the experimental results. For example, all potential models underestimate $A_y$ (the so-called $A_y$ puzzle) and $iT_{11}$ and overestimate the central minimum in $T_{21}$. Some TNF models have been constructed *ad hoc* to improve the description of these observables at low energies [27]. However, the models studied here, derived from the exchange of two pions and contact terms, are not able to solve these discrepancies. What we observed in the present study is that, after fixing the parameters of each model from the description of $B(^3\mathrm{H})$, $^2a_{nd}$, and $B(^4\mathrm{He})$, the description of the vector polarization observables lies in a narrow band, positioned differently for each model. The best description is given by the AV18 + N2LOL model, which, with respect to the original AV18 + URIX model, reduces the discrepancy in

$A_y$ and $iT_{11}$ appreciably. However, it gives a slightly worse description of the central minimum of $T_{21}$. The other two models do not improve the description of the observables, compared always to the original AV18 + URIX. The modified TM′ model gives similar results, although $iT_{11}$ is slightly worse, whereas the results with the modified URIX model are definitely worse than those with the original model. The fact that, for each model, the $A_y$ and $iT_{11}$ predictions lie in a narrow band indicates a connection between the short-range structure of the TNF and the polarization observables at low energies. From the analysis we can conclude that the smoother forms of the $y(r)$, $T(r)$, and $Z_0(r)$ functions of the N2LOL potential are preferable. It is noteworthy that the TM′ and URIX models do not include a $D$ term. An extended analysis of these two models, including one, will allow for a more stringent conclusion about the short-range structure of the TNF models. Preliminary studies in this direction are under way.

Finally, at the end of Sec. III, we analyze the $^4P_J$ phase-shift parameters. The overall attractive character of the TNF makes the $^4P_{1/2}$ and $^4P_{5/2}$ parameters larger, compared to those obtained using an $NN$ force alone, and has little effect on $^4P_{3/2}$. The mixing parameter $\epsilon_{3/2-}$ is larger too. Depending on the relative increase in these parameters, the description of $A_y$ and $iT_{11}$ can improve, as in the case of the N2LOL model, but not the description of the central minimum of $T_{21}$. The spin-isospin structure of the TNF models studied here cannot lower the $^4P_{1/2}$ phase shift, which seems to be necessary to improve the description of $T_{21}$ in the minimum. A different mechanism has to be included in the structure of the TNF, as, for example, proposed in Ref. [27]. Studies along this line are presently under way.


[1] A. Kievsky, M. Viviani, and S. Rosati, Phys. Rev. C **64**, 024002 (2001).
[2] S. A. Coon and W. Glöckle, Phys. Rev. C **23**, 1790 (1981).
[3] B. S. Pudliner, V. R. Pandharipande, J. Carlson, and R. B. Wiringa, Phys. Rev. Lett. **74**, 4396 (1995).
[4] J. L. Friar, D. Hüber, and U. van Kolck, Phys. Rev. C **59**, 53 (1999).
[5] S. A. Coon and H. K. Han, Few-Body Syst. **30**, 131 (2001).
[6] H. T. Coelho, T. K. Das, and M. R. Robilotta, Phys. Rev. C **28**, 1812 (1983); M. R. Robilotta and H. T. Coelho, Nucl. Phys. A **460**, 645 (1986).
[7] S. A. Coon and M. T. Peña, Phys. Rev. C **48**, 2559 (1993).
[8] A. Stadler, J. Adam Jr., H. Henning, and P. U. Sauer, Phys. Rev. C **51**, 2896 (1995).
[9] E. Epelbaum, A. Nogga, W. Glockle, H. Kamada, U.-G. Meissner, and H. Witala, Phys. Rev. C **66**, 064001 (2002).
[10] P. Navratil, Few-Body Syst. **41**, 117 (2007).
[11] A. C. Phillips, Nucl. Phys. A **107**, 209 (1968).
[12] P. F. Bedaque, H.-W. Hammer, and U. van Kolck, Nucl. Phys. A **646**, 444 (1999).
[13] A. Kievsky, S. Rosati, M. Viviani, L. E. Marcucci, and L. Girlanda, J. Phys. G **35**, 063101 (2008).
[14] R. B. Wiringa, V. G. J. Stoks, and R. Schiavilla, Phys. Rev. C **51**, 38 (1995).
[15] D. R. Entem and R. Machleidt, Phys. Rev. C **68**, 041001(R) (2003).
[16] A. Kievsky, M. Viviani, and S. Rosati, Nucl. Phys. A **577**, 511 (1994).
[17] A. Kievsky, Nucl. Phys. A **624**, 125 (1997).
[18] M. Viviani, A. Kievsky, and S. Rosati, Phys. Rev. C **71**, 024006 (2005).
[19] R. Lazauskas, J. Carbonell, A. C. Fonseca, M. Viviani, A. Kievsky, and S. Rosati, Phys. Rev. C **71**, 034004 (2005).
[20] M. Viviani, L. E. Marcucci, S. Rosati, A. Kievsky, and L. Girlanda, Few-Body Syst. **39**, 159 (2006).
[21] L. E. Marcucci, A. Kievsky, L. Girlanda, S. Rosati, and M. Viviani, Phys. Rev. C **80**, 034003 (2009).
[22] K. Schoen *et al.*, Phys. Rev. C **67**, 044005 (2003).
[23] S. C. Pieper, V. R. Pandharipande, R. B. Wiringa, and J. Carlson, Phys. Rev. C **64**, 014001 (2001).
[24] A. Nogga, H. Kamada, W. Glöckle, and B. R. Barrett, Phys. Rev. C **65**, 054003 (2002).
[25] S. Shimizu *et al.*, Phys. Rev. C **52**, 1193 (1995).
[26] A. Kievsky, S. Rosati, W. Tornow, and M. Viviani, Nuc. Phys. A **607**, 402 (1996).
[27] A. Kievsky, Phys. Rev. C **60**, 034001 (1999).